



Homeostatic Maintenance of Allele-Specific *p16* Methylation in Cancer Cells Accompanied by Dynamic Focal Methylation and Hydroxymethylation

Sisi Qin¹, Qiang Li¹, Jing Zhou¹, Zhao-jun Liu¹, Na Su¹, James Wilson², Zhe-ming Lu^{1*}, Dajun Deng^{1*}

¹ Key Laboratory of Carcinogenesis and Translational Research (Ministry of Education), Division of Cancer Etiology, Peking University Cancer Hospital & Institute, Beijing, China, ² GRU Cancer Center, Georgia Regents University, Augusta, Georgia, United States of America

Abstract

Aim: *p16* Methylation frequently occurs in carcinogenesis. While it has been hypothesized that the *p16* methylation states are dynamically maintained in cancer cells, direct evidence supporting this hypothesis has not been available until now.

Methods: A fusion cell model was established which reprogrammed the native DNA methylation pattern of the cells. The methylation status of the *p16* alleles was then repeatedly quantitatively analyzed in the fusion monoclonal, parental cancer cell lines (*p16*-completely methylated-AGS and unmethylated-MGC803), and HCT116 non-fusion cell using DHPLC and bisulfite sequencing. Histone methylation was analyzed using chromatin immuno-precipitation (ChIP)-PCR. P16 expression status was determined using immuno-staining and RT-PCR.

Results: The methylation status for the majority of the *p16* alleles was stably maintained in the fusion monoclonal cells after up to 60 passages. Most importantly, focal de novo methylation, demethylation, and hydroxymethylation were consistently observed within about 27% of the *p16* alleles in the fusion monoclonal cells, but not the homozygously methylated or unmethylated parental cells. Furthermore, subclones of the monoclonal cells consistently maintained the same *p16* methylation pattern. A similar phenomenon was also observed using the *p16* hemi-methylated HCT116 non-fusion cancer cell line. Interestingly, transcription was not observed in *p16* alleles that were hydroxymethylated with an antisense-strand-specific pattern. Also, the levels of H3K9 and H3K4 trimethylation in the fusion cells were found to be slightly lower than the parental AGS and MGC803 cells, respectively.

Conclusion: The present study provides the first direct evidence confirming that the methylation states of *p16* CpG islands is not only homeostatically maintained, but also accompanied by a dynamic process of transient focal methylation, demethylation, and hydroxymethylation in cancer cells.

Citation: Qin S, Li Q, Zhou J, Liu Z-j, Su N, et al. (2014) Homeostatic Maintenance of Allele-Specific *p16* Methylation in Cancer Cells Accompanied by Dynamic Focal Methylation and Hydroxymethylation. PLoS ONE 9(5): e97785. doi:10.1371/journal.pone.0097785

Editor: Jindan Yu, Northwestern University, United States of America

Received: February 6, 2014; **Accepted:** April 22, 2014; **Published:** May 14, 2014

Copyright: © 2014 Qin et al. This is an open-access article distributed under the terms of the Creative Commons Attribution License, which permits unrestricted use, distribution, and reproduction in any medium, provided the original author and source are credited.

Funding: This work is supported by National Natural Science Foundation of China [Grant 31261140372 and 81171900], National Basic Research Program of China [Grant 2011CB504201 and 2010CB529303], and Beijing Natural Science Foundation of China [Grant 7122033]. The funders had no role in study design, data collection and analysis, decision to publish, or preparation of the manuscript.

Competing Interests: Dajun Deng is a PLOS ONE Editorial Board member. This does not alter the authors' adherence to PLOS ONE Editorial policies and criteria.

* E-mail: zheminglu@163.com (ZML); dengdajun@bjmu.edu.cn (DD)

Introduction

DNA methylation is considered to be one of the most stable epigenetic modifications in mammals. The methylation states of cell differentiation related genes have been shown to be highly dynamic during germ cell and preimplantation development, but become relatively static during the development of somatic tissues [1–3]. In contrast, the methylation states of host adaptation related genes remain dynamic in somatic tissues in order to allow for the proper response to environmental factor exposure and subsequent pathogenesis [4–6]. Hydroxymethylation of DNA is intimately involved in altering gene methylation status and has been found to not only play a key role in DNA demethylation, but also serve many of its own functions [7,8].

Tumor suppressor P16 encoded by the *ink4/arf* locus within human chromosome 9p21 is a cell cycle regulator involved in the

inhibition of G1 → S phase transition through the P16-CDK4/6-RB pathway [9]. The locus is transcriptionally silenced in embryonic stem cells, and plays a rate-limiting role in the reprogramming of induced pluripotent cells [10]. Although a 9p21 fragment deletion is the most frequent genetic alteration found in all cancers [11], hypermethylation of CpG islands is still the main mechanism for *p16* inactivation in multiple human cancers [12–14]. In fact, a number of cohort studies have shown that *p16* methylation occurs early in carcinogenesis and has been shown to significantly increase the risk of malignant transformation of epithelial dysplasia [15–21]. Even though the causative role of *p16* methylation in carcinogenesis has not been established, the evidence strongly suggests that *p16* methylation may contribute significantly to cancer development and could be developed into a potential biomarker [4]. Although *p16* methylation is one of the most highly studied epigenetic modifications, its stability in cancer

cells and the mechanism through which it is maintained has not yet been clarified [22–26]. A detailed understanding of the maintenance machinery involved in DNA methylation is a critical step for the development of methylation biomarkers and epigenetic intervention therapy.

The prevalence of p16 methylation in human chronic gastritis tissues is strongly correlated with *Helicobacter pylori* infection, and dramatically decreased after *H. pylori* eradication, suggesting that most methylated-p16 alleles may not be stable [27,28]. In contrast, p16 methylation in cultured normal and cancer cells is likely very stable as it was efficiently recovered after the DNA methylation inhibitor (5-aza-CdR) was removed [29]. However, reactivation of methylation-silenced genes was observed in a certain proportion of the DNA methyltransferase inhibitor-treated cells. It is difficult to exclude the possibility that the observed recovery of p16 methylation results from a selection advantage conferred to cells that do not undergo p16 reactivation/demethylation during the inhibitor treatment. In addition, it has recently been reported that methylated CpG sites within the p16 CpG islands are mainly located in the p16 exon-1 coding nucleosomal region in human gastritis lesions and extend into the 5'UTR and promoter nucleosomal regions during the development of gastric carcinomas [26]. These findings suggest that the fully methylated-p16 alleles might be more stable than the focally methylated alleles; however, this hypothesis should be further tested using monoclonal cells containing p16 alleles with diverse methylation patterns, including focal methylation.

Cell fusion has been used to study the mechanisms behind gene transcription regulation and DNA methylation alteration [24,30]. In order to establish a cell model containing diverse p16 methylation patterns, a gastric cancer cell line with completely methylated p16 (AGS) was combined with a p16-active gastric cancer cell line (MGC803) through cell fusion. Next, these fusion cells were cloned and subcloned before the distribution of methylated and hydroxymethylated CpG sites within the p16 CpG islands was characterized. The methylation status of most p16 alleles in the fusion cells remained the same as the parental cells. Low levels of focal de novo methylation, demethylation, and hydroxymethylation were also observed in the fusion cells; however, these changes were found to be instable events. A similar phenomenon was also observed using the p16 hemimethylated cell line HCT116. These findings indicate that the methylation states of p16 CpG islands are homeostatically maintained in cancer cells. To the best of our knowledge, this is the first report to suggest that the methylation status of CpG islands is homeostatically maintained in cancer cells not undergoing differentiation.

Materials and Methods

Cell culture

Human gastric cancer cell line MGC803 was cultured in RPMI 1640 medium with 10% FBS. AGS was cultured in F12 medium with 10% FBS. MGC803 [31] and AGS (ATCC CRL-1739) cell lines were kindly provided by Prof. Yang Ke at Peking University Cancer Hospital and Institute. HCT116 cells were kindly provided by Dr. Yuanjia Chen, Peking Union Hospital (ATCC CCL-247), and were cultured in RPMI 1640 medium with 10% FBS.

Generation of the stable fusion cell clones

pBabe-puro (hygromycin resistance) and pIRES2-EGFP (neomycin/G418 resistance) vectors were transfected to AGS and MGC803 cells, respectively, using Lipofectamine™ 2000 (Invitrogen, 11668-027) according to the manufacturer's instruction.

Puromycin (puromycin^{res}-AGS) and G418 (neomycin^{res}-MGC803) selection was performed on AGS and MGC803 cell lines followed by culture in F12 medium with 10% FBS and puromycin (0.25 µg/mL) and RPMI 1640 medium with 10% FBS and neomycin (700 µg/mL), respectively. The fusion was performed using PEG8000 as described previously [32]. After fusion, the cells were cultured in selection medium containing both neomycin (700 µg/mL) and puromycin (0.25 µg/mL). Following selection, individual colonies were mono-cloned, and after three rounds of subsequent cloning, five monoclonal cells were obtained. Two of the five monoclonal cells were chosen for further mono-cloning.

Microsatellites D9S974 and D9S1749 analysis

The primer set for D9S974 (sense, 5'-gagcc tggct tggat cataa-3'; antisense, 5'-aagct tacag aacca gacag-3') and D9S1749 (sense, 5'-aggag agggt acgtg tgcaa-3'; antisense, 5'-tacag ggtgc gggcg agatg aa-3') were used to amplify the p16 alleles (Figure S1A). Genotypes of the microsatellites were analyzed at 80°C by DHPLC using a UV detector (260 nm) as described previously [33].

Karyotype analysis

A 25-cm flask at 60% cell confluence was treated with 0.2 µg/mL colchicine for 4 hrs. Cells were recovered after trypsinization and treatment with 75 mmol/L KCl solution for 25 min. The cells were fixed (3:1 methanol: acetic acid), and stained with Giemsa stain.

DNA preparation, bisulfite and TAB treatment

Genomic DNA was extracted from tissue samples with phenol/chloroform. The samples were treated with 5 mol/L of sodium bisulfite for 16 hrs at 50°C [34]. For 5hmC analysis, genomic DNA was treated using the TAB Kit according to manufacturer's specifications (WiseGene, Cat# K001) [35].

Hydroxymethylated DNA-specific immunoprecipitation (hMeDIP)

Genomic DNA was sonicated into 200 bp to 600 bp fragments using Bioruptor sonicator (Diagenode). 100 ng sonicated DNA was saved as the input control. Each sample consisted of 1 µg sonicated DNA diluted in IP buffer and incubated with 4 µl anti-hydroxymethylcytosine (5hmC) antibody (Active Motif) at 4°C overnight. The antibody-DNA complexes were captured using protein A/G beads then purified. PCR was run on all samples using 35 cycles with the primers 5'-agtcct ccttc ctgc caac-3' and 5'-tccga gcact tagcg aatgt g-3'. Unmethylated cytosine, 5-methylcytosine, and 5hmC DNA fragments were used as PCR controls to verify 5hmC enrichment.

Chromatin-immunoprecipitation (ChIP) assays

Levels of histone modifications H3K9me3 and H3K4me3 were determined using ChIP assays as described [36].

PCR amplifications

The 392 bp amplicon of the antisense-strand of the p16 exon-1 was amplified with the CpG-free primer set (sense, 5'-ttttt agagg attg aggga tagg-3'; antisense, 5'-ctacc taatt ccaat tccc taca acttc-3') as described [37]. The 588 bp amplicon of the antisense-strand of the p16 exon-1 and promoter was amplified using the sMSP primer set (sense, 5'-ctactt aattc caatt cccct aca-3'; antisenses, 5'-ccaat tccc taca acttc g-3', 5'-ccaat tccc taca acttc atct ccaa atcg-3' and 5'-ccaat tccc taca acttc atct ccaa atcac ccg-3') [26]. The 369 bp of the sense-strand of the p16 exon-1 was amplified with the CpG-free primer set (sense, 5'-gttgt agatt tttta

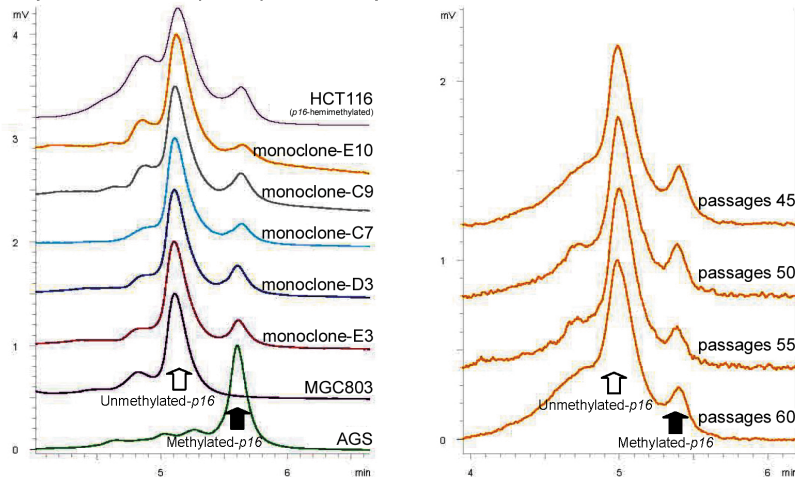
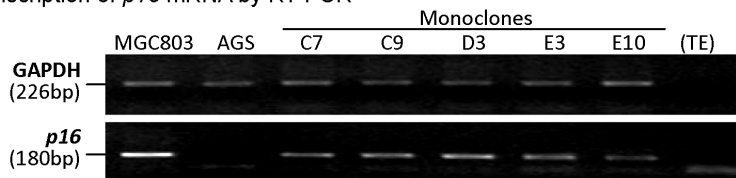
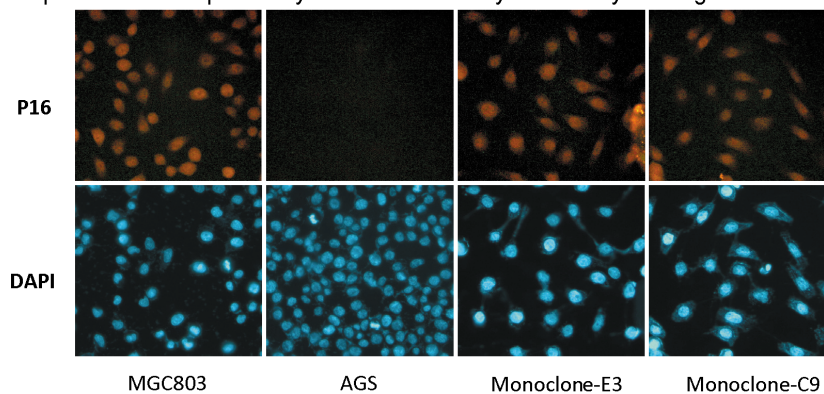
A: Methylation status of *p16* CpG island by DHPLC at 57.6°C**B: Transcription of *p16* mRNA by RT-PCR****C: Expression of P16 protein by confocal immunocytochemistry staining**

Figure 1. Characterization of methylation and expression of *p16* in the fusion cell lines. (A) The methylation states of *p16* CpG islands in the fusion mono-clones were analyzed using DHPLC (left). The proportion of methylated-*p16* in the mono-clone-E10 was stably maintained at passages 45, 50, 55, and 60 (right). (B) RT-PCR shows varying mRNA expression of *p16* in the fusion mono-clones and their parental MGC803 and AGS cell lines. (C) Confocal immunocytochemistry staining shows varying P16 expression in the various cell lines. doi:10.1371/journal.pone.0097785.g001

tttat ttgga t-3'; antisense, 5'-tcccc ttacc taaaa aaata cc-3') at annealing temperature 56°C. The 284 bp and 346 bp amplicons of the antisense-strands of the *p16* exon-2 and intron-2 were respectively amplified with the CpG-free primer set (sense, 5'-tggtg ggta tgatg atggg ag-3'; antisense, 5'-aacat aatta ctacc tctaa tacc c-3') and (sense, 5'-tttgt gggtt tgtag aagta ggtat g-3'; antisense, 5'-ctaa tcaa caactaatcc actac c-3') at annealing temperature 57°C.

Methylation quantification of CpG islands using DHPLC

The 392 bp, 369 bp, 284 bp, 346 bp PCR products amplified by universal primers were separated using the WAVE DNA Fragment Analysis System with a fluorescence (FL)-detector (Transgenomic, Inc., OM, USA) at 57.6, 55.0, 58.0, and 57°C, respectively [37,38]. The WAVE-HS1 FL-dye buffer (Transgenomic, Inc.) was used to enhance the FL-intensity of PCR

products (universal post-column labelling). Genomic HCT116 DNA was used as standard control.

Clone sequencing

PCR was performed on the bisulfite converted DNA. The amplicons were cloned into the pCR-blunt vector (Invitrogen), transformed into *E. coli*, and sequenced using an ABI 3730 Analyzer.

***p16* RT-PCR**

p16 mRNA was detected as described [12].

P16 immunofluorescence staining

Immunofluorescence staining was performed as previously described [39]. In short, fusion cells were fixed in 4% formalde-

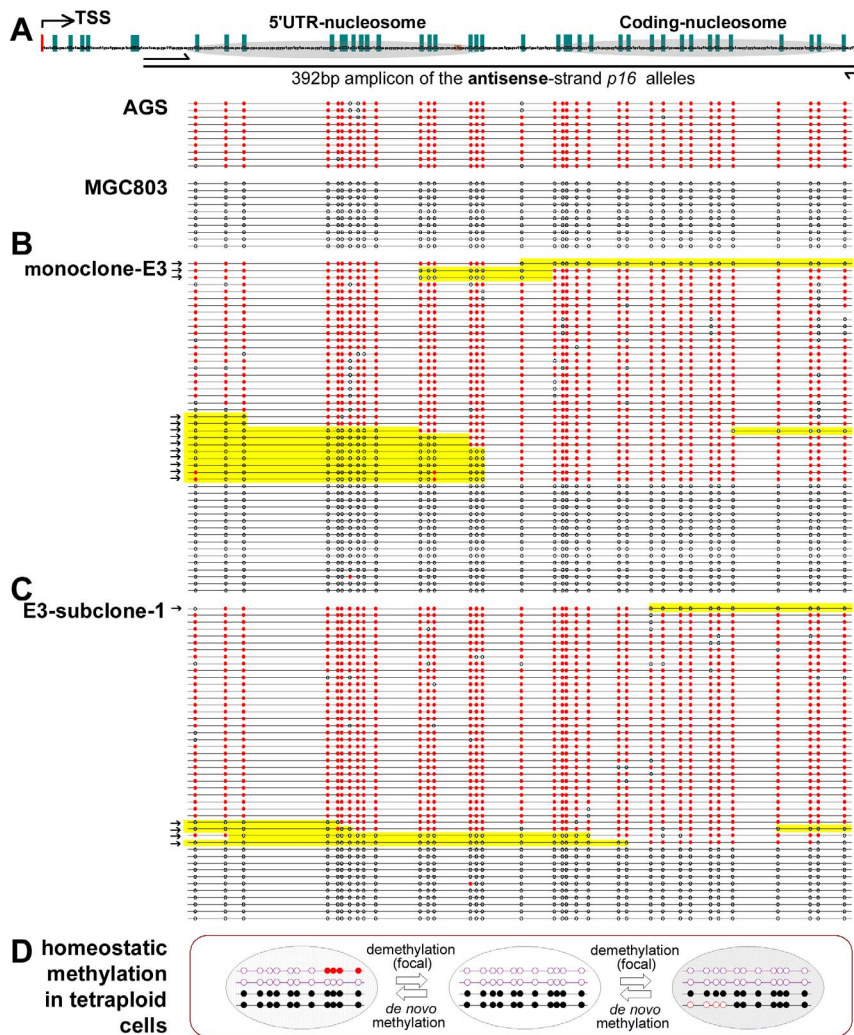


Figure 2. Bisulfite sequencing of *p16* alleles in the fusion cells and their parental cells. (A) Bisulfite clone sequencing of the 392 bp fragment of the *p16* CpG island in AGS and MGC803 cells; Each green bar represents a CpG site. Nucleosomal location in exon-1 is also marked (26). (B and C) Bisulfite sequencing in the fusion monoclonal-E3 and subclones. Focal methylation changes (yellow-shadowed); methylated CpG sites (red dot); unmethylated CpG sites (open dot); focally methylated- or demethylated-*p16* molecules (black arrows). (D) Homeostatic methylation model for a single CpG island in the tetraploid cells.
doi:10.1371/journal.pone.0097785.g002

hyde/PBS for 10 min before a 5-min wash in PBS. Fixed samples were blocked for 30 min with 0.5% Triton X-100/PBS at room temperature. Cells were incubated with anti-P16 antibody (Abcam, ab54210) for 1 h at 37°C, after washed with 0.5% Triton X-100/PBS, then incubated with goat-anti rabbit IgG antibody labeled with rhodamine for 1 h at 37°C. DAPI (1:2000) was used to stain the cell nucleus. Photos were taken on a Leica confocal microscope.

Results

Establishment and characterization of a cell fusion model with diversely methylated *p16* alleles

It has been reported that heterokaryons can induce DNA methylation variation via cell fusion of two cell lines [30]. We hypothesized that a cell fusion model containing different methylation states of *p16* CpG islands could duplicate the de novo methylation or demethylation processes. Thus, puromycin⁺-AGS cells containing fully methylated-*p16* alleles and the

neomycin⁺-MGC803 cells containing unmethylated-*p16* alleles were constructed, respectively. These two cell lines were then fused and cultured in selection medium containing both puromycin and neomycin. After three rounds of cloning, the fusion monoclonal cells were characterized using two microsatellites (D9S974 and D9S1749) near the *p16* locus (Figure S1A). Two D9S1749 microsatellite chromatogram patterns (C7/C9/E10 and D3/E3) and one D9S974 pattern were observed in 5 tested monoclonal cells that differed from the patterns of their parental cells. Chromosome mode was also different between the representative clone E10 (near-tetraploid) and its parental cells (near-diploid) (Figure S1B).

Stable maintenance of completely methylated and unmethylated-*p16* alleles in cancer cells

The methylation status of the *p16* CpG islands (392 bp) was quantitatively analyzed in these fusion clones using a DHPLC assay as previously reported [37]. As was seen in the *p16* hemimethylated HCT116 cells, the ratio of methylated- to unmethylated-*p16* molecules was about 1:1 in these fusion clones

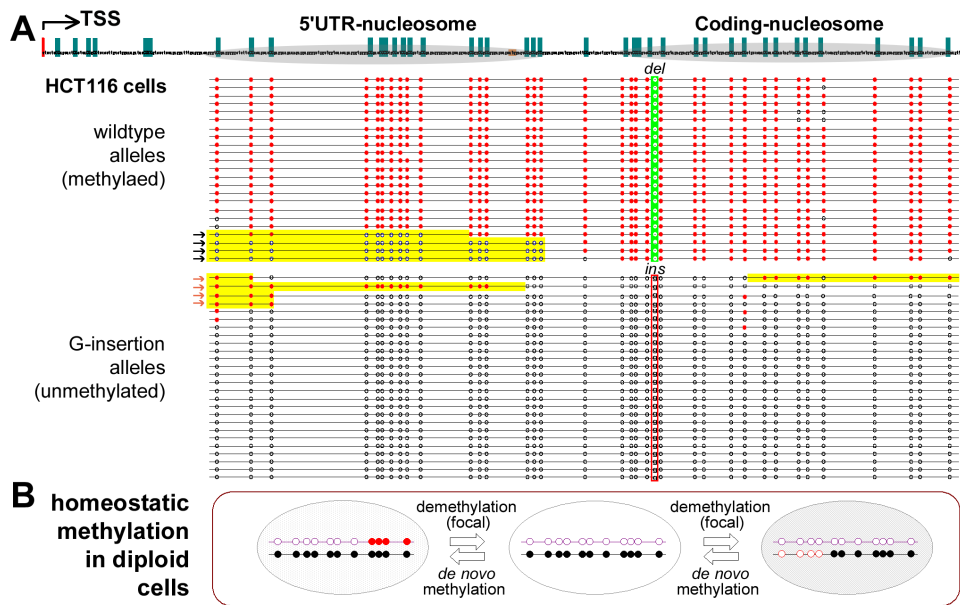


Figure 3. Bisulfite sequencing of *p16* alleles in HCT116 cells. (A) Bisulfite clone sequencing of the 392 bp fragment of the *p16* CpG island in HCT116 cells. Wild-type (*deletion*)/mutant (*G-insertion*) *p16* alleles; focally demethylated-*p16* molecules (black arrows); focally *de novo* methylated molecules (red arrows). (B) Homeostatic methylation model for a single CpG island in the diploid cells. doi:10.1371/journal.pone.0097785.g003

(Figure 1A-left). The proportion of methylated-*p16* alleles was stably maintained in a representative clone from passages 45, 50, 55, and 60 (Figure 1A-right). Furthermore, RT-PCR detected *p16* mRNA in all 5 tested clones (Figure 1B). Nucleoplasmic *p16* protein was also observed within each cell in two representative monoclonal cells (C9 and E3) (Figure 1C). Based on this information, it is evident that the transcription/methylation states of the *p16* alleles in the fusion cells is likely maintained in a similar pattern to their parental cells.

Focally methylated *p16* alleles are not stable in cancer cells

Interestingly, while most *p16* molecules remained in the completely methylated or unmethylated states, the representative fusion clones contained about 27% (13/48) focally methylated- (or demethylated-) *p16* molecules in the exon-1 region (Figure 2B). However, the homozygously methylated or unmethylated parental cells did not exhibit the same methylation changes. In order to confirm that the tested clone was in fact monoclonal, this clone was further subcloned. Further analysis revealed that the *p16* methylation patterns in two subclones consistently remained similar to their parental clones (Figure 2C and Figure S2).

A single nucleotide polymorphism (SNP) (rs36228836) was identified in the *p16* promoter region. It was determined that the genotype of this SNP differed between the two parental cell lines (T/A for MGC803 and T/T for AGS), thus making it possible to identify the MGC803-specific *p16* A-alleles in the fusion cells (Figure S3). In order to clarify whether these focally methylated fragments were the result of *de novo* methylation or demethylation, the methylation states within a 588 bp fragment covering this SNP were analyzed using a seeding methylation-specific PCR assay (sMSP). It was discovered that CpG methylation of the *p16* alleles at the methylation “seeding” sites within intron-1 were effectively enriched [26]. Results of bisulfite-sequencing confirmed that focal *de novo* methylation was observed in the MGC803-specific A-alleles of monoclonal-D3 (Figure S3).

In order to investigate whether the transient focally methylated-*p16* alleles exist in non-fusion cells, the methylation pattern of the *p16* hemi-methylated HCT116 cell line was also analyzed. Similarly, 16% (8/49) of the *p16* molecules showed focal methylation in the HCT116 cells (Figure 3). Furthermore, by using a *del/ins* reading frame-shift mutation found in the exon-1 coding region as a genetic marker, it was determined that both focal *de novo* methylation in the mutant *G-insertion* alleles (mainly unmethylated) and demethylation in the wild-type alleles (mainly methylated) also occur sporadically in the HCT116 cells (4/26 and 4/23, respectively). This indicates that the focal methylation and demethylation of *p16* alleles do in fact exist in non-fusion cancer cells. Taken together, these results suggest that while focal methylation and demethylation are relatively common events, most of the completely methylated- and unmethylated-*p16* alleles are stably maintained in cancer cells.

In order to study whether the focal methylation/demethylation occurs in the gene body, we analyzed the methylation states of CpG islands within the *p16* exon-2 and intron-2. DHPLC analysis revealed that these two CpG islands were fully methylated in AGS, MGC803, and HCT116 cells (Figure S4A&B), and bisulfite-sequencing of the intron-2 CpG island confirmed the DHPLC results (Figure S4C), suggesting the gene body is homogeneously and stably methylated in these cells and is not accompanied focal methylation/demethylation.

Concomitant 5-hydroxymethylation occurs in the *p16* alleles of fusion cells

DNA methylation and hydroxymethylation cannot be readily differentiated using regular bisulfite-based methylation assays. The role of hydroxymethylation in the focal *p16* methylation or demethylation was investigated using hMeDIP-PCR assay (Figure 4A, left chart). The results of this assay showed that the amount of hydroxymethylated-*p16* DNA in the two fusion clones was significantly higher than their parent cells (Figure 4A, right chart).

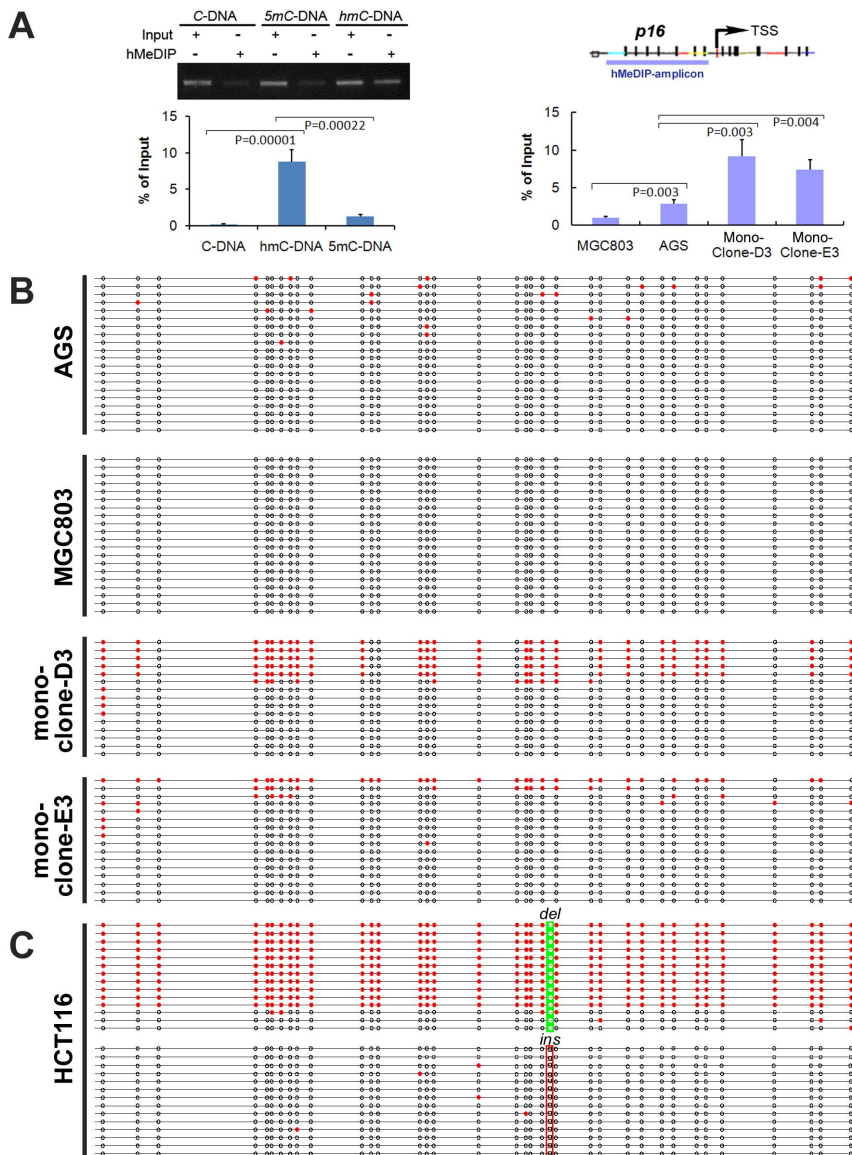


Figure 4. *p16* chromatin hydroxymethylation characterization. (A) Immuno-precipitation and PCR analysis of synthetic and cellular 5hmC-containing *p16* sequences. The AGS and fusion monoclone-D3 and E3 cells show significant levels of 5hmC. (B) TAB-seq analysis reveals completely hydroxymethylated-*p16* alleles in the fusion subclones, but not the parental cells. (C) TAB-seq analysis of HCT116 cells shows the majority of the wildtype *p16* alleles are completely hydroxymethylated. doi:10.1371/journal.pone.0097785.g004

Tet-assistant bisulfite sequencing (TAB-seq) is capable of specifically detecting 5-hydroxy-methylcytosine (5hmC) in DNA at a single base resolution [35]. Using this assay to analyze the 5hmC content in the *p16* CpG islands in details, it was found that AGS cells exhibit sporadic hydroxymethylated CpGs at a very low frequency (21/700), while the MGC803 cells did not show any hydroxymethylation. As expected, both complete and focal hydroxymethylation of *p16* alleles were detected in these fusion cells (Figure 4B). The results of two assays consistently indicate that hydroxymethylation may play a role in the homeostatic maintenance of *p16* methylation in the fusion cells.

Analysis of HCT116 cells unexpectedly revealed frequent and complete hydroxymethylation within the antisense-strands of the *p16* wildtype (del) alleles (11/14), but not in the G-insertion mutant alleles (Figure 4C). While methylation was detected in the 369 bp fragment of the sense-strand of the *p16* exon-1 in HCT116

cells as expected (Figure 5A–C), notably, the complete hydroxymethylation was not observed in the sense-strands in both TAB-DHPLC analysis and TAB-sequencing (Figure 5C and D), suggesting the antisense strand specific hydroxymethylation.

In order to determine if the completely hydroxymethylated wildtype *p16* alleles are transcriptionally active, the allele-origin of the sequencing revealed that none of the 48 *p16* mRNA molecules were transcribed from wildtype *p16* alleles that were asymmetrically methylated and hydroxymethylated (M:H) (Figure 6). This information proves that hydroxymethylation in the antisense strand of the *p16* alleles may not lead to transcriptional activation of the gene.

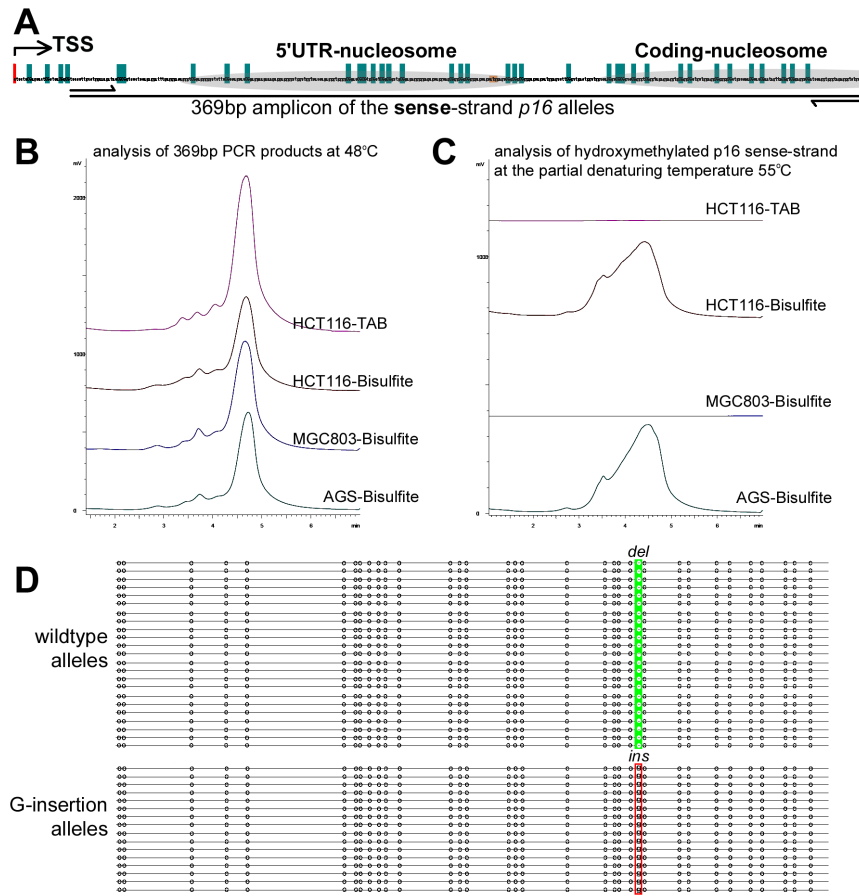


Figure 5. Analysis of hydroxymethylation in the sense-strand of *p16* CpG island in HCT116 cells. (A) Location of the 369 bp amplicon of the sense-strand *p16* exon-1. (B) Detection of the 369 bp PCR products using DHPLC (sizing mode) at 48°C. (C) Detection of hydroxymethylated molecules amplified from the *p16* sense-strand after TAB modification using DHPLC (FL detector) at the partial denaturing temperature 55°C. Under this condition, the hydroxymethylated- and unhydroxymethylated-*p16* molecules are partially and completely denatured, respectively. The regular bisulfite-treated templates are used as reference controls. (D) Results of TAB-sequencing for the 369 bp PCR products amplified from HCT116 cells. doi:10.1371/journal.pone.0097785.g005

Concomitant of histone H3K4 and H3K9 trimethylation at the *p16* alleles in fusion cells

ChIP-PCR was used to quantitatively determine the levels of active H3K4me3 and repressive H3K9me3 in the fusion cells (Figure 7). The H3K4me3 level in the heterogeneously methylated *p16* alleles of the fusion subclones was found to be significantly lower than was seen in the completely unmethylated alleles of the MGC803 cells. Furthermore, the level of H3K4me3 in exon-1 chromatin was determined to be higher than was found in promoter chromatin. While the H3K4me3 was not detected in the AGS cells, the H3K9me3 level was significantly higher in this cell line than other cell lines. H3K9me3 level showed an inverse correlation with the H3K4me3 level among these cell lines.

Discussion

The DNA methylation pattern is known to change dynamically during the differentiation of embryonic stem cells and development of tissues in vertebrates. However, it remains a mystery how the methylation states of the genome are maintained in cells no longer undergoing differentiation. In the present study, it was found that the methylation states of completely methylated- and unmethylated-*p16* alleles remained stable during cell proliferation. Furthermore, low levels of focal demethylation, hydroxymethyla-

tion, and *de novo* methylation occurred relatively frequently in two kinds of *p16* hemi-methylated cancer cell models, but not in homogeneously methylated or unmethylated cells. These findings imply that homogeneous methylation can exert repression pressure on the *p16* gene that can at least partially affect formerly unmethylated CpG islands. In contrast, the transcription pressure exerted by complete demethylation of the gene is capable of inducing and maintaining demethylation of *p16* CpG islands. Hydroxymethylation of *p16* CpG alleles was also discovered to play a role in the homeostatic maintenance of genome methylation. To our knowledge, this is the first report to show that the methylation status of a tumor suppressor gene is homeostatically maintained in cancer cells.

The stability of methylated *p16* alleles has not yet been explained. In gastritis lesions, the methylation states of most *p16* alleles are unstable and *H. pylori*-dependent [27,28]; however, in cancer cell lines they have proven to remain remarkably stable [29]. Our recent comprehensive sequencing studies revealed that the methylated CpG sites in gastritis are located within the exon-1 region of the *p16* gene, but extend into the promoter region after the development of gastric carcinoma. This implies that completely methylated-*p16* alleles are considerably more stable than their focally methylated counterparts [26]. It has also been reported that heterokaryons can induce DNA methylation

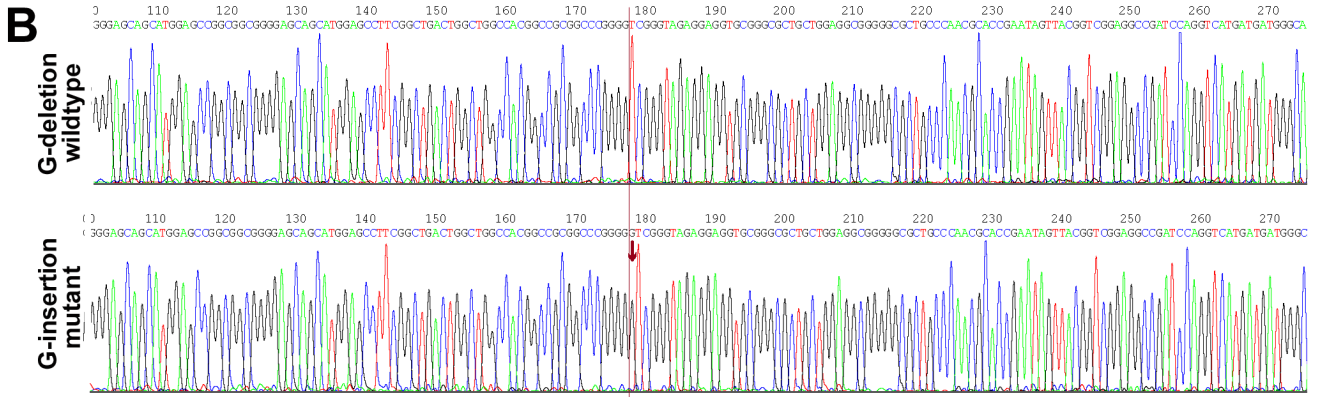
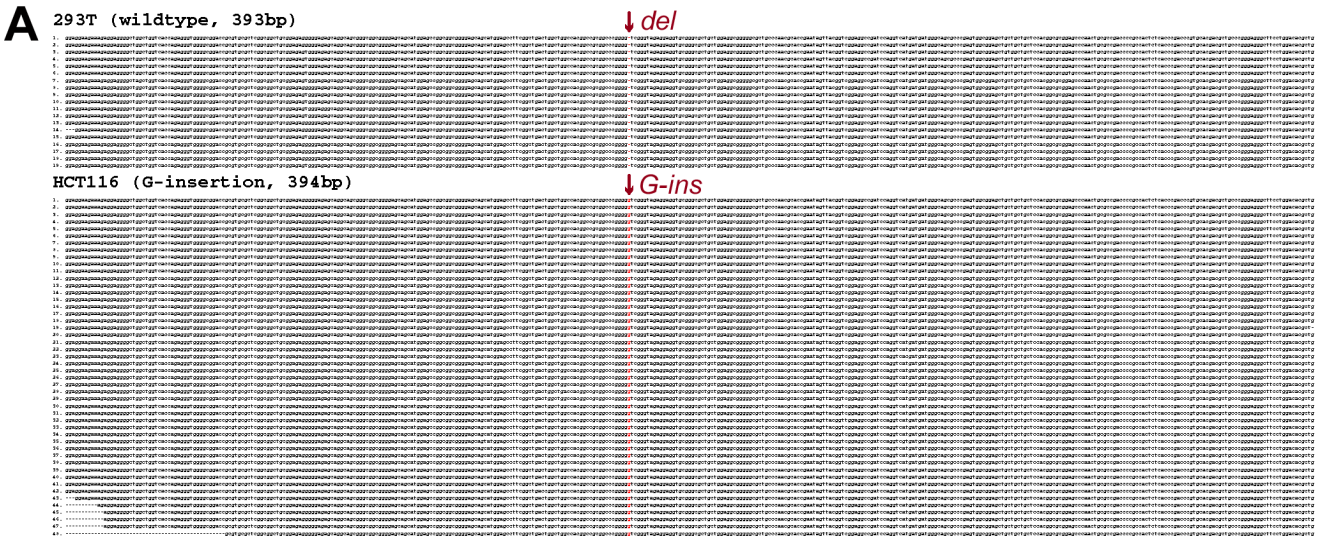


Figure 6. Allele specific RT-PCR analysis of *p16* mRNA of cells. (A) RT-PCR clone sequencing of the control 293T cell line (del) shows wildtype *p16* mRNA. The HCT116 (G-ins) cell line revealed only mutant *p16* mRNA clones. (B) Clone sequencing results show both wildtype and mutant *p16* mRNA.

doi:10.1371/journal.pone.0097785.g006

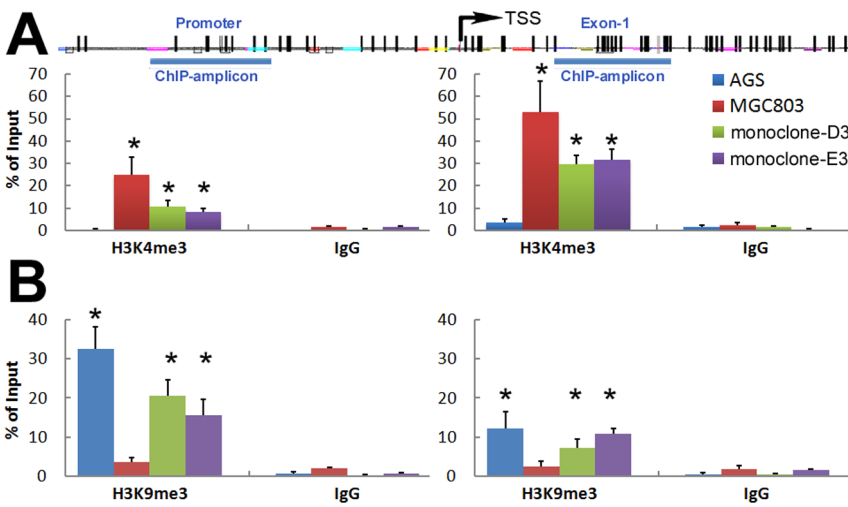


Figure 7. Characterization of histone modifications in the *p16* chromatin by ChIP-PCR assays. (A) The active H3K4me3 level within the *p16* CpG islands in the fusion subclones and MGC803 cells was significantly higher than AGS cells, especially in the exon-1 region (monoclonals vs. AGS, $P < 0.01$). (B) The repressive H3K9me3 level in the fusion subclones and AGS cells was significantly higher than MGC803 cells, especially in the promoter region (monoclonals vs. MGC803, $P < 0.01$).

doi:10.1371/journal.pone.0097785.g007

variations via cell fusion of two cell lines, and furthermore that some silenced-*p16* molecules in mouse cancer cells can be reactivated after being fused with *p16*-active mouse embryonic stem cells [30,39]. In the present study, fusion cells containing a wide variety of *p16* methylation patterns were established from homozygously methylated and unmethylated parental cell lines in order to investigate the stability of focally and completely methylated-*p16* alleles within the same cell. As expected, the *p16* alleles of the fusion cells showed a complete and variable range of methylation. The *p16* alleles in the fusion clones and their subclones remained stably hemi-methylated during cell passages, which indicate that these completely methylated and unmethylated *p16* alleles are relatively stable. On the other hand, hemi-methylated fusion clones and HCT116 cells exhibited low levels of focally methylated/demethylated-*p16* alleles, which provide direct evidence that the hemi-methylated *p16* alleles are less stable than the homogeneously methylated *p16* alleles. This dynamic, but still homeostatic, methylation pattern of *p16* CpG islands may offer a common mechanism explaining DNA methylation maintenance in differentiation static cells. In addition, two CpG islands in the *p16* exon-2 and intron-2 are homogeneously methylated in HCT116, AGS, and MGC803 cells, hence it is likely the homeostatic maintenance of *p16* methylation could be observed only in its promoter/exon-1 region in these cells. Because there are many hemi-methylated regions present in the genome, such as the X-chromosomes of female cells and imprinted genes, further study as to whether focal, transient methylation and demethylation are general phenomena in homeostatic maintenance of DNA methylation is certainly warranted.

5hmC plays a crucial role in active DNA demethylation as an intermediate in serial methylcytosine oxidation. However, a certain proportion of 5hmC is not further oxidized, but is instead maintained in the genome of adult tissues such as the brain and colon. Although the additional functions of 5hmC in the genome remain unknown, it is likely to serve an important purpose. It has been reported that hydroxymethylation at both promoter and intragenic locations correlated positively with gene expression [40]. Generally, CpG islands are not methylated in regions around transcription start sites in actively transcribed genes, but are methylated in the gene body. Recently, it has been reported that hydroxymethylation in the genome of the brain is TET2-dependent and more hydroxymethylation is detected in the sense-strands than the antisense-strands of actively transcribed gene bodies [41,42]. In the present study, we found that the antisense-strands of HCT116 cells contained a certain proportion of “methylated” wildtype *p16* alleles that were actually completely hydroxymethylated; but the corresponding sense-strands were not hydroxymethylated. It indicates that hydroxymethylation around the transcription start site in the completely methylated *p16* wildtype alleles may be an antisense-strand-specific phenomenon. Further analysis revealed that the asymmetrically methylated and hydroxymethylated (M:H) wildtype *p16* alleles were rendered transcriptionally inactive. It is needed to study whether hydroxymethylation bias toward the antisense-strand is a universal event for all promoter/exon-1 regions in the genome where hydroxymethylation occurs.

References

1. Wu H, Zhang Y (2011) Tet1 and 5-hydroxymethylation: a genome-wide view in mouse embryonic stem cells. *Cell Cycle* 10: 2428–2436.
2. Hackett JA, Surani MA (2013) DNA methylation dynamics during the mammalian life cycle. *Philos Trans R Soc Lond B Biol Sci* 368: 20110328.
3. Hahn MA, Qiu R, Wu X, Li AX, Zhang H, et al. (2013) Dynamics of 5-hydroxymethylcytosine and chromatin marks in Mammalian neurogenesis. *Cell Rep* 3: 291–300.
4. Deng D, Liu Z, Du Y (2010) Epigenetic alterations as cancer diagnostic, prognostic, and predictive biomarkers. *Adv Genet* 71: 125–176.
5. Thomson JP, Hunter JM, Lempiäinen H, Müller A, Terranova R, et al. (2013) Dynamic changes in 5-hydroxymethylation signatures underpin early and late events in drug exposed liver. *Nucleic Acids Res* 41: 5639–5654.

While considerably more research will have to be performed to fully elucidate the fine details behind genomic methylation status maintenance, we successfully identified and characterized key differences in inheritance patterns between complete- and hemi-methylated-*p16* alleles in both fusion and colon cancer cell lines. In conclusion, the current study illustrated that the states of completely methylated and unmethylated-*p16* alleles are homeostatically maintained in differentiation static cancer cells with concomitant transient focal *de novo* methylation, hydroxymethylation, and demethylation.

Supporting Information

Figure S1 DHPLC characterization of fusion mono-clones using two microsatellite markers located within the MTAP-*p16*/Arf/*p15* locus at chromosomal region 9q21.

(A) The genotypes of the fusion clones differ from their parental cells at both D9S1749 and D9S974. (B) Analysis of chromosome mode for the fusion monoclonal-E10 and their parental cells. The number of cells containing a different number of chromosomes is displayed on the left. The chromosome mode was 92 for the fusion clone, 58 for MGC803 cells, and 46 for AGS cells.

(TIF)

Figure S2 Effect of 5-aza-CdR (5 μ M) or TSA (0.1 μ M) alone and in combination on proliferation of the fusion and parental cells.

Both the fusion cells and MGC803 cells are very sensitive to the inhibitory effects of TSA, while the AGS cells showed lower sensitivity.

(TIF)

Figure S3 Bisulfite sequencing of *p16* alleles in the fusion subclone cells and their parental cells.

Seeding methylation-specific PCR (sMSP) analysis of the 588 bp fragments of the *p16* CpG islands methylated at one of the three seeding sites in intron-1 (26). Each row represents a *p16* molecule; CpG sites (black bar); methylated CpG sites (●); unmethylated CpG sites (○); genotype *p16* alleles at SNP rs36228836 (A or T); focally *de novo* methylated *p16* molecules in the sub-subclone E3 (red arrows).

(TIF)

Figure S4 Characterization of the methylation states of CpG islands in the *p16* exon-2 and intron-2.

(A and B) DHPLC analysis reveals that the exon-2 and intron-2 CpG islands are completely methylated in two representative fusion clones, their parental MGC803 and AGS cells, and HCT116 cells. (C) Bisulfite-sequencing shows that the intron-2 CpG islands are homogeneously methylated in these cells. (D) Locations of three CpG islands within the *p16* allele are illustrated.

(TIF)

Author Contributions

Conceived and designed the experiments: DD ZML. Performed the experiments: SQ QL JZ ZJL NS ZML. Analyzed the data: SQ QL ZML DD. Contributed reagents/materials/analysis tools: JZ ZJL. Wrote the paper: SQ JW ZML DD.

6. Deng DJ, Lu ZM (2013) Differentiation and adaptation epigenetic networks: Translational research in gastric carcinogenesis. *Chinese Science Bulletin* 58: 1–6.
7. Song CX, He C (2013) Potential functional roles of DNA demethylation intermediates. *Trends Biochem Sci* 38: 480–484.
8. Spruijt CG, Gnerlich F, Smits AH, Pfaffeneder T, Jansen PW, et al. (2013) Dynamic readers for 5-(hydroxy)methylcytosine and its oxidized derivatives. *Cell* 152: 1146–1159.
9. Serrano M, Hannon G, Beach D (1993) A new regulatory motif in cell-cycle control causing specific inhibition of cyclin D/CDK4. *Nature* 366: 704–707.
10. Li H, Collado M, Villasante A, Strati K, Ortega S, et al. (2009) The Ink4/Arf locus is a barrier for iPSC cell reprogramming. *Nature* 460: 1136–1139.
11. Beroukhi R, Mermel CH, Porter D, Wei G, Raychaudhuri S, et al. (2010) The landscape of somatic copy-number alteration across human cancers. *Nature* 463: 899–905.
12. Merlo A, Herman JG, Mao L, Lee DJ, Gabrielson E, et al. (1995) 5' CpG Island Methylation Is Associated with Transcriptional Silencing of the Tumor-Suppressor P16/CDKN2/MTS1 in Human Cancers. *Nature Medicine* 1: 686–692.
13. Herman JG, Merlo A, Mao L, Lapidus RG, Issa JPJ, et al. (1995) Inactivation of the CDKN2/P16/MTS1 Gene Is Frequently Associated with Aberrant DNA Methylation in All Common Human Cancers. *Cancer Research* 55: 4525–4530.
14. Gonzalez-Zulueta M, Bender CM, Yang AS, Nguyen T, Beart RW, et al. (1995) Methylation of the 5' CpG island of the p16/CDKN2 tumor suppressor gene in normal and transformed human tissues correlates with gene silencing. *Cancer Res* 55: 4531–4535.
15. Belinsky SA, Nikula KJ, Palmisano WA, Michels R, Saccomanno G, et al. (1998) Aberrant methylation of p16(INK4a) is an early event in lung cancer and a potential biomarker for early diagnosis. *Proceedings of the National Academy of Sciences of the United States of America* 95: 11891–11896.
16. Bai H, Gu LK, Zhou J, Deng DJ (2003) p16 hypermethylation during gastric carcinogenesis of Wistar rats by N-methyl-N'-nitro-N-nitrosoguanidine. *Mutation Research-Genetic Toxicology and Environmental Mutagenesis* 535: 73–78.
17. Sun Y, Deng DJ, You WC, Bai H, Zhang L, et al. (2004) Methylation of p16 CpG islands associated with malignant transformation of gastric dysplasia in a population-based study. *Clinical Cancer Research* 10: 5087–5093.
18. Belinsky SA, Liechty KC, Gentry FD, Wolf HJ, Rogers J, et al. (2006) Promoter hypermethylation of multiple genes in sputum precedes lung cancer incidence in a high-risk cohort. *Cancer Research* 66: 3338–3344.
19. Hall G, Shaw R, Field E, Rogers S, Sutton D, et al. (2008) p16 Promoter methylation is a potential predictor of malignant transformation in oral epithelial dysplasia. *Cancer Epidemiol Biomarkers Prev* 17: 2174–2179.
20. Cao J, Zhou J, Gao Y, Gu LK, Meng HX, et al. (2009) Methylation of p16 CpG Island Associated with Malignant Progression of Oral Epithelial Dysplasia: A Prospective Cohort Study. *Clinical Cancer Research* 15: 5178–5183.
21. Jin Z, Cheng Y, Gu W, Zheng Y, Sato F, et al. (2009) A multicenter, double-blinded validation study of methylation biomarkers for progression prediction in Barrett's esophagus. *Cancer Res* 69: 4112–4115.
22. Wong DJ, Foster SA, Galloway DA, Reid BJ (1999) Progressive region-specific de novo methylation of the p16 CpG island in primary human mammary epithelial cell strains during escape from M(0) growth arrest. *Mol Cell Biol* 19: 5642–5651.
23. Hinshelwood RA, Melki JR, Huschtscha LI, Paul C, Song JZ, et al. (2009) Aberrant de novo methylation of the p16INK4A CpG island is initiated post gene silencing in association with chromatin remodelling and mimics nucleosome positioning. *Hum Mol Genet* 18: 3098–3109.
24. Yao JY, Zhang L, Zhang X, He ZY, Ma Y, et al. (2010) H3K27 trimethylation is an early epigenetic event of p16INK4a silencing for regaining tumorigenesis in fusion reprogrammed hepatoma cells. *J Biol Chem* 285: 18828–18837.
25. Li Q, Wang X, Lu Z, Zhang B, Guan Z, et al. (2010) Polycomb CBX7 Directly Controls Trimethylation of Histone H3 at Lysine 9 at the p16 Locus. *Plos One* 5.
26. Lu ZM, Zhou J, Wang X, Guan Z, Bai H, et al. (2012) Nucleosomes Correlate with In Vivo Progression Pattern of De Novo Methylation of p16 CpG Islands in Human Gastric Carcinogenesis. *PLoS One* 7: e35928.
27. Dong CX, Deng DJ, Pan KF, Zhang L, Zhang Y, et al. (2009) Promoter methylation of p16 associated with Helicobacter pylori infection in precancerous gastric lesions: A population-based study. *International Journal of Cancer* 124: 434–439.
28. Perri F, Cotugno R, Piepoli A, Merla A, Quitadamo M, et al. (2007) Aberrant DNA methylation in non-neoplastic gastric mucosa of H. Pylori infected patients and effect of eradication. *Am J Gastroenterol* 102: 1361–1371.
29. Egger G, Aparicio AM, Escobar SG, Jones PA (2007) Inhibition of histone deacetylation does not block resiliency of p16 after 5-aza-2'-deoxycytidine treatment. *Cancer Research* 67: 346–353.
30. Bhutani N, Brady JJ, Damian M, Sacco A, Corbel SY, et al. (2010) Reprogramming towards pluripotency requires AID-dependent DNA demethylation. *Nature* 463: 1042–1047.
31. Wang KH (1983) A in vitro cell line (MGc80-3) of a poorly differentiated mucoid adenocarcinoma of human stomach. *Acta Biol Exp Sinica (J Mol Cell Biol)* 16: 257–267.
32. Silva J, Chambers I, Pollard S, Smith A (2006) Nanog promotes transfer of pluripotency after cell fusion. *Nature* 441: 997–1001.
33. Pan KF, Liu W, Lu YY, Zhang L, Li ZP, et al. (2003) High throughput detection of microsatellite instability by denaturing high-performance liquid chromatography. *Hum Mutat* 22: 388–394.
34. Eads CA, Danenberg KD, Kawakami K, Saltz LB, Blake C, et al. (2000) MethylLight: a high-throughput assay to measure DNA methylation. *Nucleic Acids Res* 28: E32.
35. Yu M, Hon GC, Szulwach KE, Song CX, Jin P, et al. (2012) Tet-assisted bisulfite sequencing of 5-hydroxymethylcytosine. *Nat Protoc* 7: 2159–2170.
36. Kim S, Nollen EA, Kitagawa K, Bindokas VP, Morimoto RI (2002) Polyglutamine protein aggregates are dynamic. *Nat Cell Biol* 4: 826–831.
37. Luo D, Zhang B, Lv L, Xiang S, Liu Y, et al. (2006) Methylation of CpG islands of p16 associated with progression of primary gastric carcinomas. *Lab Invest* 86: 591–598.
38. Deng DJ, Deng GR, Smith MF, Zhou J, Xin HJ, et al. (2002) Simultaneous detection of CpG methylation and single nucleotide polymorphism by denaturing high performance liquid chromatography. *Nucleic Acids Research* 30: 13E.
39. Zhang B, Xiang S, Zhong Q, Yin Y, Gu L, et al. (2012) The p16-Specific Reactivation and Inhibition of Cell Migration Through Demethylation of CpG Islands by Engineered Transcription Factors. *Human Gene Therapy* 23: 1071–1081.
40. Bhattacharyya S, Yu Y, Suzuki M, Campbell N, Mazdo J, et al. (2013) Genome-wide hydroxymethylation tested using the HELP-GT assay shows redistribution in cancer. *Nucleic Acids Res* 41: e157.
41. Lister R, Mukamel EA, Nery JR, Urich M, Puddifoot CA, et al. (2013) Global epigenomic reconfiguration during mammalian brain development. *Science* 341: 1237905.
42. Wen L, Li X, Yan L, Tan Y, Li R, et al. (2014) Whole-genome analysis of 5-hydroxymethylcytosine and 5-methylcytosine at base resolution in the human brain. *Genome Biol* 15: R49.